Clinical Trial/Experimental Study

Medicine®

OPEN

Functional prediction of miR-3144-5p in human cardiac myocytes based on transcriptome sequencing and bioinformatics

Lei Ruan, MD, PhD, Yi Yang, MS, Yi Huang, MS, Ling Ding, MS, Cuntai Zhang, MD, PhD, Xiaofen Wu, MD, PhD*

Abstract

Background: RAN guanine nucleotide release factor (*RANGRF*) encoding protein MOG1 plays an important role in cardiac arrhythmia, so we intended to investigate the regulatory miRNA of *RANGRF* and explore its potential regulatory mechanism in arrhythmogenesis.

Methods: Based on bioinformatic analysis, miR-3144-5p was predicted to be a regulatory miRNA of *RANGRF*, which were then validated through a dual-luciferase reporter plasmid assay. Subsequently, the expression level of miR-3144-5p in human cardiac myocytes (HCMs) was detected, followed by cell transfection with miR-3144-5p mimics. Transcriptome sequencing was then performed in HCMs with or without transfection. The sequencing results were subjected to bioinformatic analyses, including differentially expressed gene (DEG) analysis, functional enrichment analysis, protein–protein interaction (PPI) network analysis, miRNA-target gene analysis, and miRNA-transcription factor (TF)-target gene coregulatory network analysis.

Results: There really existed a regulatory relation between miR-3144-5p and *RANGRF*. The expression level of miR-3144-5p was low in HCMs. After cell transfection, miR-3144-5p expression level significantly increased in HCMs. Bioinformatic analyses of the transcriptome sequencing results identified 300 upregulated and 271 downregulated DEGs between miR-3144-5p mimic and control group. The upregulated genes *ISL1* and neuregulin 1 (*NRG1*) were significantly enriched in cardiac muscle cell myoblast differentiation (GO:0060379). *CCL21* was one of the hub genes in the PPI network and also a target gene of miR-3144-5p. Moreover, the TF of v-Myc avian myelocytomatosis viral oncogene neuroblastoma-derived homolog (MYCN) was involved in the miR-3144-5p-TF-target gene coregulatory network and interacted with the target genes of miR-3144-5p.

Conclusion: *ISL1*, *NRG1*, *CCL21*, and MYCN were differentially expressed in the miR-3144-5p mimic group, suggesting that miR-3144-5p overexpression plays a role in HCMs by regulating these genes and TF. This study may provide new insight into the mechanisms behind the progression of cardiac arrhythmia.

Abbreviations: CCL21 = C-C motif chemokine ligand 21, DEG = differentially expressed gene, GO = Gene Ontology, HCM = human cardiac myocyte, ISL1 = ISL LIM homeobox 1, KEGG = Kyoto Encyclopedia of Genes and Genomes, MYCN = v-Myc avian myelocytomatosis viral oncogene neuroblastoma-derived homolog, NES = normalized enrichment score, NRG1 = neuregulin 1, PPI = protein–protein interaction, RANGRF = RAN guanine nucleotide release factor, STRING = Search Tool for the Retrieval of Interacting Genes/Proteins, TF = transcription factor, UTR = untranslated region, WNT4 = Wnt family member 4.

Keywords: bioinformatics, cardiac arrhythmia, human cardiac myocyte, miR-3144-5p, transcriptome sequencing

Editor: Anastasios Lymperopoulos.

Funding/support: This work was supported by The independent innovation research fund of Huazhong University of Science and Technology (Program No.2017KFYXJJ131) and the Specialized Research Fund for the Doctoral Program of Higher Education from the Ministry of Education (Program No.20130142120068).

The authors have no conflicts of interest to disclose.

Department of Gerontology, Tongji Hospital, Tongji Medical College, Huazhong University of Science and Technology, Wuhan, Hubei, China.

** Correspondence: Xiaofen Wu, Department of Gerontology, Tongji Hospital, Tongji Medical College, Huazhong University of Science and Technology, Jie Fang Da Dao 1095#, Wuhan, Hubei 430030, China (e-mail: wux2018@sina.com).*

Medicine (2017) 96:32(e7539)

Received: 24 February 2017 / Received in final form: 23 June 2017 / Accepted: 26 June 2017

http://dx.doi.org/10.1097/MD.0000000000007539

Key Points

1. miR-3144-5p is a target gene of *RANGRF*.
2. A total of 571 genes are differentially expressed between miR-3144-5p mimic and control groups.
3. *ISL1* and *NRG1* were enriched in cardiac muscle cell myoblast differentiation.
4. *CCL21* is one of the hub genes in the PPI network.
5. MYCN is involved in the miR-3144-5p-TF-target gene coregulatory network.

1. Introduction

Cardiovascular diseases are the most common cause of mortality and morbidity worldwide.[1] Among cardiovascular diseases, cardiac arrhythmia is a group of conditions in which the heart beat is irregular, including tachycardia (a heart rate more than

100 beats/min in adults) and bradycardia (a heart rate less than 60 beats/min). Most types of cardiac arrhythmia are not serious, but some types can predispose an individual to complications such as heart failure, stroke, or cardiac arrest, which are risk factors for life-threatening cardiac arrhythmias.[2] Unfortunately, the molecular mechanisms underlying life-threatening cardiac arrhythmias have remained unclear until recently.

A recent study demonstrated a functional role for small noncoding RNAs (microRNAs) in the pathophysiology of cardiac arrhythmia.[3] miRNAs are a group of small noncoding RNAs, mainly acting as suppressors of gene expression at the posttranscriptional level by binding to the 3′-untranslated region (UTR) of target mRNAs,[4] the aberrant expression of which has been implicated in numerous diseases, including arrhythmogenesis.[5,6] miR-3144 is a recently identified miRNA located in the E6-encodingregion, which is reported to be dysregulated in several types of cancer.[7–9] To our knowledge, its role in cardiovascular disease has not been reported. Interestingly, based on miRecord, a publicly available bioinformatic tool,[10] miR-3144-5p was predicted to be a regulatory miRNA of RAN guanine nucleotide release factor (*RANGRF*), the gene encoding MOG1.[11]

MOG1 is a 187-amino-acid protein that can interact with intracellular loop II (between DII and DIII) of the pore-forming α subunit of the cardiac voltage-gated Na^+ channel complex ($Na_v1.5$), which is important for impulse conduction in the heart.[11] The overexpression of MOG1 was shown to cause significant increases in $Na_v1.5$ cell surface expression and whole-cell cardiac sodium currents.[12] $Na_v1.5$ is encoded by the sodium voltage-gated channel alpha subunit 5 (*SCN5A*) gene, and mutations in *SCN5A* have been associated with cardiac arrhythmias, such as atrial fibrillation, Brugada syndrome, and long QT syndrome.[13] Therefore, MOG1 may be involved in the progression and development of cardiac arrhythmia.

Given the importance of MOG1 in cardiac arrhythmia, we speculated that the regulatory miRNAs of *RANGRF* may also play a role in arrhythmogenesis. Therefore, in this study, we first used a dual-luciferase reporter plasmid assay to verify the regulatory relationship between miR-3144-5p and *RANGRF* in human cardiac myocytes (HCMs). Then, we performed transcriptome sequencing and bioinformatic analyses to further investigate the functions of miR-3144-5p in HCMs. This study may provide a new insight into the mechanisms of arrhythmogenesis.

2. Materials and methods

2.1. Cell culture and transfection

The primary HCMs (6200) used in this study were purchased from ScienceCell (Carlsbad, CA), maintained in Dulbecco's modified Eagle's medium, and passaged by trypsinization. Then, cells at 70% confluence were seeded in 6-well plates before transfection. After 16 hours, cells were transfected with miR-3144-5 mimics and an miRNA mimic negative control (NC) using Lipofectamine 2000 (Invitrogen, Gaithersburg, MD), which was then confirmed by a real-time polymerase chain reaction (PCR) assay.

2.2. Real-time PCR assay

miR-3144-5p expression in HCMs was detected using real-time PCR. Briefly, total RNA was extracted using RNA Iso-plus reagent (9019; Takara, Beijing, China). After measurement of the RNA concentration and purity, cDNA was synthesized using TIANscript RT Kit (KR201-01; Takara, Beijing, China). PCR amplification was performed using the SYBR Green PCR method, in accordance with the instructions of the SYBR Premix Ex Taq™ Kit (Takara, Beijing, China). Each reaction was performed in triplicate. U6 was used as an internal control: U6-F, 5′-CTCGCTTCGGCAGCACA-3′ and U6-R, 5′-AACGCTTCACGAATTTGCGT-3′. The primers used for miR-3144-5p amplification were as follows: forward, 5′-AGGGGACCAAAGAGATATATAG-3′ and reverse, 5′-GCTGTCAACGATACGCTACCTA-3′.

2.3. Construction of luciferase reporter gene recombinant plasmid

Based on *RANGRF* gene sequences in the National Center for Biotechnology Information database (https://www.ncbi.nlm.nih.gov/), the primers of RANGRF-3A-UTR were designed and synthesized by Sangon Biotech (Shanghai, China). The restriction enzyme cutting sites were added to the 5′ hend of primers. The primers were as follows: 4741RANGRF-F (XhoI), 57-AAGATCGCCGTGTGACTCGAGTCTCTTGCTTACCTT-CAATCAGCC-3a, and 4741RANGRF-R (XbaI), 5′-AAGATCTGCGGCCGCTCTAGATATATTGATTATAAAG-CAAGTTTATTCTGAAGAGG-3A. The *RANGRF* gene was amplified by PCR. Then, the products of PCR and the luciferase reporter plasmid pGL3 (Promega, Madison, WI) were digested using XhoI and XbaI. After measuring the concentrations of the target fragment and vector, they were recombined by seamless cloning. The products were then transformed into competent *Escherichia coli* cells and subjected to DNA sequencing to select a luciferasereporter gene recombinant plasmid.

2.4. Dual-luciferase reporter plasmid assay

For the luciferase reporter assay, HCMs were plated in 96-well plates and cotransfected with luciferase reporter vectors. The pRL-TK plasmid containing the *Renilla* luciferase gene (Promega) was used as a normalizing control. After 48 hours of incubation, cells were lysed and assayed for luciferase activity using the Dual-Luciferase Reporter Assay System (Promega), in accordance with manufacturer's instructions.

2.5. RNA purification, library preparation, and sequencing

Four samples, including 2 normal HCMs (control group: Con 1 and Con 2) and 2 transfected HCMs (test group: T1 and T2), were subjected to sequencing. Specifically, total RNA was extracted using Trizol (15596-018; Invitrogen); its integrity was verified using 2% agarose gel electrophoresis, while its quality and purity were evaluated using a spectrophotometer. Then, mRNA was isolated from 5 μg of total RNA using the NEBNext Poly (A) mRNA Magnetic Isolation Module (NEB #E7490) and fragmented into small pieces (200 nt). The 1st-strand cDNA was synthesized using random hexamer primers. The cDNA was then converted into double-stranded cDNA, which was subsequently subjected to end repair, phosphorylation, dA tailing, and adaptor ligation. Finally, the cDNA library was generated, quantitated using quantitative PCR, and then sequenced on the Illumina HiSeq2500 platform.

The data are available at ftp://119.57.118.228 (username: shfhxx_lxs; password: ANCR0304).

2.6. Primary processing of raw reads and annotation of transcription

The obtained raw reads were quality-filtered by removing the adaptor sequences and ambiguous or low-quality reads. The obtained clean reads were aligned to the human reference genome (hg19) using TopHat2.0.8 (http://tophat.cbcb.umd.edu/) with its default parameters. Based on human gene annotation information contained in the GeneCode database, the count values of reads of each gene were obtained using HTSeq-count 0.6.1p2 (http://www-huber.embl.de/users/anders/HTSeq). Finally, the read count matrices of 4 samples were identified.

2.7. Differentially expressed gene (DEG) analysis

The read count data were normalized based on the trimmed mean of M values of the edgeR[14,15] package and then converted into a gene expression matrix with the voom[16] method in the limma[17,18] package. Voom can convert read count data into log2-counts per million, which can calculate the differences in expression levels between control and test groups using the linear model approach in the limma package. We calculated *P*-values regarding the significance of differences using moderated t-statistics. Cut-off values of *P*-value $<.05$ and $|\log_2 (\text{fold change})| \geq 0.58$ were applied. The heatmap of DEGs was drawn using the Complex Heatmap[19] package in R.

2.8. Functional enrichment analyses

Based on the obtained DEGs, Gene Ontology (GO), including biological process, molecular function, and cellular component categories, and Kyoto Encyclopedia of Genes and Genomes pathway enrichment analyses were carried out using the Database for Annotation, Visualization, and Integrated Discovery online tool (http://david.abcc.ncifcrf.gov/).[20] Enrichment of GO functions and Kyoto Encyclopedia of Genes and Genomes pathways by at least 2 DEGs with a *P*-value $<.05$ indicated significant enrichment results.

2.9. Protein–protein interaction (PPI) network analysis

PPI analysis can help reveal the principles by which functional cellular networks are organized and provide new insights into protein functions.[21] Therefore, we constructed a PPI network for further analysis of the DEGs. The Search Tool for the Retrieval of Interacting Genes/Proteins (STRING, http://string-db.org/)[22] can predict the interactions among proteins encoded by the DEGs. The prediction methods of the STRING database come from Co-occurrence, Neighborhood, Co-expression Experiments, Gene Fusion, TextMining, and Database views. After inputting the DEGs into STRING, the PPI pairs were output to construct the PPI network using Cytoscape (http://www.cytoscape.org/) software.[23]

2.10. Analysis of topological features of nodes in PPI network

Most biological networks obey scale-free attribution.[24] The important nodes in the PPI network were analyzed based on 3 methods of calculation of network topological features: degree centrality,[25] betweenness centrality,[26] and closeness centrality.[27] The topology scores of nodes in the PPI network were calculated using the CytoNCA[28] plugin of Cytoscape. The nodes with higher scores (hub nodes) may play important roles in the PPI network.

2.11. Analysis of target genes of miR-3144-5p

The target genes of miR-3144-5p were predicted by the target module of the Mirwalk2 (http://zmf.umm.uni-heidelberg.de/apps/zmf/mirwalk2/) database.[29] The predicted miRNA-gene interaction pairs should appear in all 4 databases, namely miRWalk, miRanda, RNA22, and Targetscan 4. Subsequently, DEGs were selected from the predicted target genes to construct the miR-3144-5p-target DEG regulatory network.

2.12. miR-3144-5p-transcription factor (TF)-gene coregulatory network analysis

Based on the iRegulon[30] plugin of Cytoscape, the TFs that regulate the target genes of miR-3144-5p were predicted. The parameter settings for iRegulon were minimum identity between orthologous genes:0.05, and maximum false discovery rate on motif similarity:0.001. The output results included normalized enrichment score (NES). A higher NES indicated a more reliable result. TF-target gene pairs with NES >3 were selected in this study.

A study found that there were direct or indirect interactions between miRAN and TFs.[31] Enright et al[31] found that TFs were more likely to be targets of miRAN than normal genes. In this context, in this study TFs were selected from the target genes of miR-3144-5p, and miR-3144-5p-TF interaction pairs were obtained. Finally, TF-target gene interaction pairs and miR-3144-5p-TF interaction pairs were combined to construct the coregulatory network of miR-3144-5p-TF-gene.

2.13. Statistical analysis

Statistical analysis was conducted using SPSS 16.0 (SPSS, Inc., Chicago, IL). Data are expressed as mean ± standard error of the mean. Differences were analyzed using *t* test. Differences with $P < .05$ were considered statistically significant.

3. Results

3.1. miR-3144-5pis a direct regulatory miRNA of RANGRF

The bioinformatic tool miRecord predicted that miR-3144-5p is a regulatory miRNA of *RANGRF*. Dual-luciferase reporter plasmid assay was also used to confirm thatmiR-3144-5pbinds to the 3′-UTR of *RANGRF* mRNA. As shown in Fig. 1, miR-3144-5p significantly decreased the luciferase expression of 3′-UTR-RANGRF, suggesting that miR-3144-5pisa direct regulatory miRNA of *RANGRF* ($P < .05$).

3.2. miR-3144-5p was low in HCMs

The expression level of miR-3144-5p in HCMs was determined by qRT-PCR and was found to be low. However, after HCMs had been transfected with miR-3144-5p mimics, the relative expression level of miR-3144-5p increased significantly compared with that in the control ($P < .01$) (Fig. 2).

3.3. RNA-Seq data analysis

After Illumina HiSeq2500 sequencing, we obtained a global overview of the transcriptome of HCMs transfected withmiR-3144-5p mimics (T1 and T2)/NC (Con 1 and Con 2). The 4 samples had raw reads numbering between 40,925,500 and 42,600,828 with raw bases ranging from 6,138,825,000 to 6,390,124,200. After stringent filtration, 40,141,128,

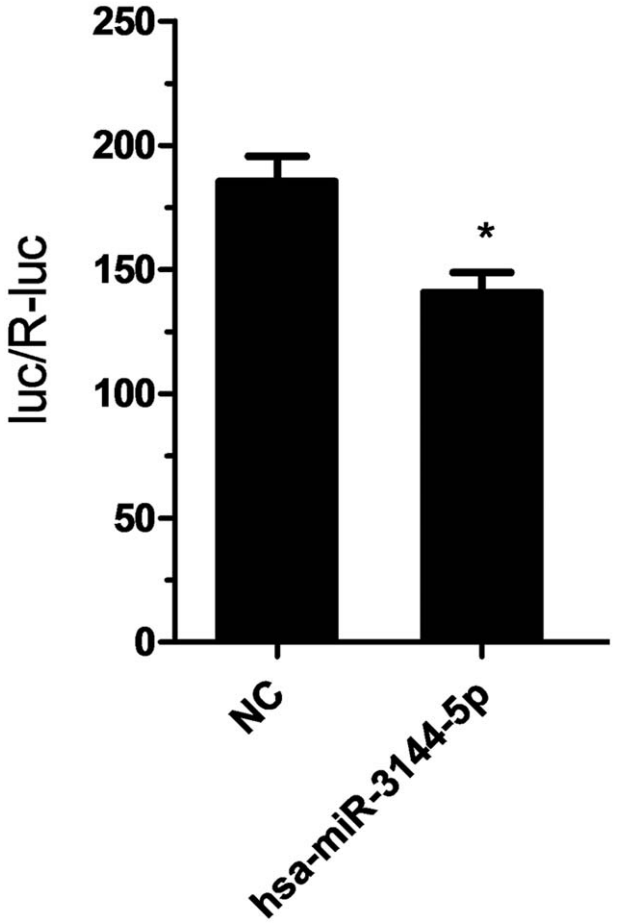

Figure 1. The relative luciferase activity of miR-3144-5p detected using the dual-luciferase reporter plasmid assay. $^{*}P < .05$ compared to the negative control group.

40,014,762, 41,730,062, and 40,184,634 clean reads were obtained in T1, T2, Con 1, and Con 2, respectively. After mapping reads to the reference genome, we obtained the following read-mapping rates: the left end ranging from 91.96% to 92.58% and the right end ranging from 87.50% to 88.10%.

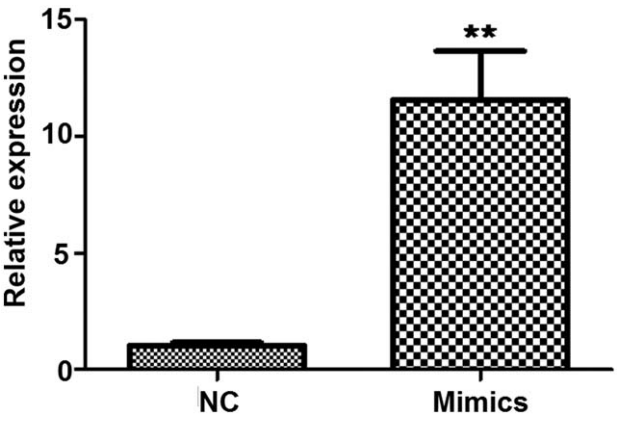

Figure 2. The relative expression level of miR-3144-5p in human cardiac myocytes after transfection, as determined by real-time polymerase chain reaction (RT-PCR). $^{**}P < .01$ compared to the negative control group.

3.4. DEG analysis

Based on the thresholds of a *P*-value $<.05$ and $|\log_2 (\text{fold change})| \geq 0.58$, a total of 571 DEGs (300 upregulated and 271 downregulated) were obtained in the test group compared with the levels in the control group. The heatmap for these DEGs is shown in Fig. 3.

3.5. Functional enrichment analyses

As shown in Fig. 4A, the upregulated DEGs were significantly enriched in the signaling pathways regulating the pluripotency of stem cells (hsa04550), the Hippo signaling pathway (hsa04390), and the Hedgehog signaling pathway (hsa04340). In particular, the upregulated ISL LIM homeobox 1 (*ISL1*) and neuregulin 1 (*NRG1*) were enriched in cardiac muscle cell myoblast differentiation (GO:0060379). The downregulated DEGs were significantly enriched in immunological synapse formation (GO:0001771), integral component of membrane (GO:0016021), and TGF-beta signaling pathway (hsa04350) (Fig. 4B).

3.6. PPI network analysis

A PPI network that comprised 255 nodes and 191 PPI pairs was constructed (Fig. 5). The top 25 nodes (hub nodes) with high topology scores are shown in Table 1. Among these nodes, 15 gene nodes appeared 3 times because their topology scores in the 3 centrality methods were among the top 25, which included proopiomelanocortin (*POMC*), Wnt family member 4 (*WNT4*), Indian hedgehog (*IHH*), and C-C motif chemokine ligand 21 (*CCL21*). Functional enrichment analysis of these 15 genes revealed that they were associated with cell–cell signaling (GO:0007267), extracellular space (GO:0005615), receptor agonist activity (GO:0048018), and signaling pathways regulating the pluripotency of stem cells (hsa04550) (Table 2).

3.7. Analysis of target genes of miR-3144-5p

A total of 15 target genes of miR-3144-5p were predicted, including 7 upregulated (*TMEM145*, *CST7*, *APOL4*, *DISC1*, *ARHGDIG*, *FAM110C*, and *MUC12*) and 8 downregulated ones (*GRTP1*, *PCDHGC4*, *CXorf36*, *SMOC1*, *RIMBP3*, *HOXB6*, *CCL21*, and *ALOXE3*). The constructed miR-3144-5p-target gene regulatory network is shown in Fig. 6.

3.8. miR-3144-5p-TF-targetgene coregulatory network analysis

The miR-3144-5p-TF-target gene co-regulatory network was constructed (Fig. 7). This network included 11 DEGs (*HOXB6*, *CXorf36*, *CCL21*, *DISC1*, *ARHGDIG*, *RIMBP3*, *ALOXE3*, *GRTP1*, *MUC12*, *CST7*, and *SMOC1*) and 11 TFs (BCL3, ETV6, HMGA1, HOXA10, JUNB, KDM4C, KLF5, v-Myc avian myelocytomatosis viral oncogene neuroblastoma-derived homolog [MYCN], NFIC, POU2F3, and SREBF2).

4. Discussion

This study revealed that miR-3144-5p is a regulatory miRNA of *RANGRF*. Owing to the low expression level of miR-3144-5p in HCMs, we performed transfection with miR-3144-5p mimics to induce its overexpression in HCMs and then performed transcriptome sequencing. Bioinformatic analyses of the transcriptome sequencing results identified 300 upregulated and 271

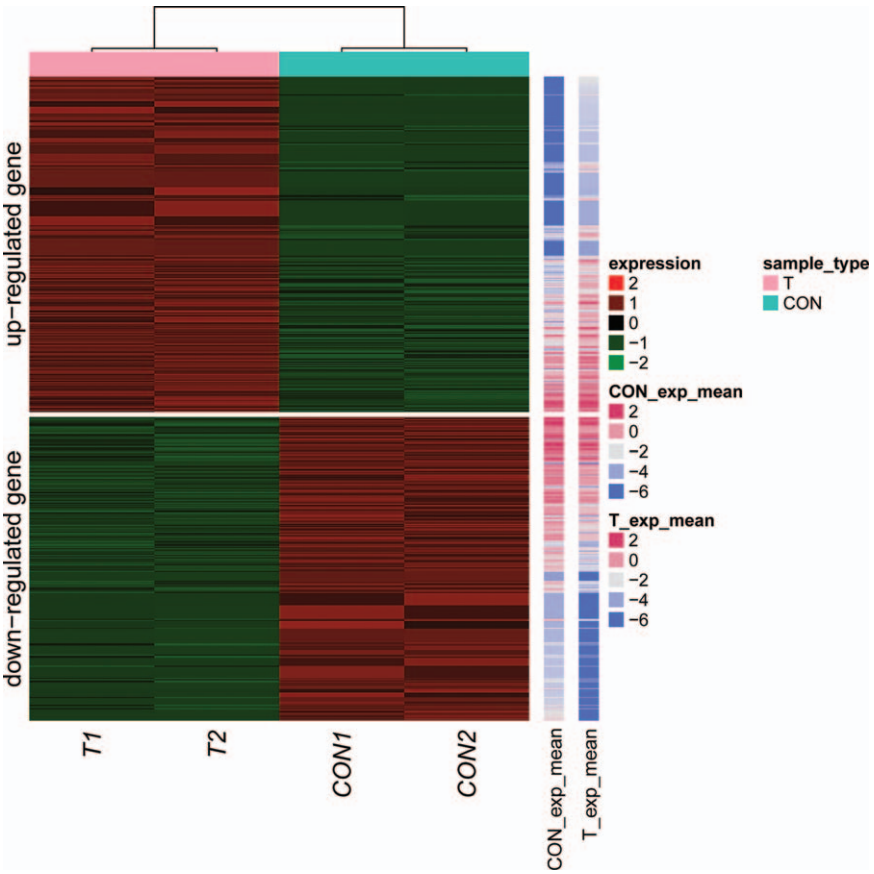

Figure 3. Heatmap plot of differentially expressed genes across all samples. Columns represent genes and rows represent samples.

downregulated DEGs. Among these, *ISL1* and *NRG1* were significantly enriched in cardiacmuscle cell myoblast differentiation (GO:0060379). *CCL21* was found to be a hub gene in the PPI network and also a target gene of miR-3144-5p. The TF MYCN is involved in the miR-3144-5p-TF-target gene coregulatory network and interacted with the target genes of miR-3144-5p.

miRNAs have emerged as ubiquitous regulators of a plethora of physiological and pathophysiological processes in cells.[32] Numerous studies have implicated miRNAs in cardiovascular physiology and the onset of cardiovascular disease.[33,34] Additionally, Santulli et al[3] reported that miRNAs regulated several properties of cardiac physiology and excitability, including automaticity, Ca^{2+} handling, conduction, and repolarization. In particular, a recent study unveiled an essential role of miRNAs in regulating cardiac arrhythmogenesis.[35] The present study suggested that dysregulation of miR-3144-5p in HCMs induced hundreds of genes to be differently expressed, which may indicate the importance of miR-3144-5p in cardiac physiology.

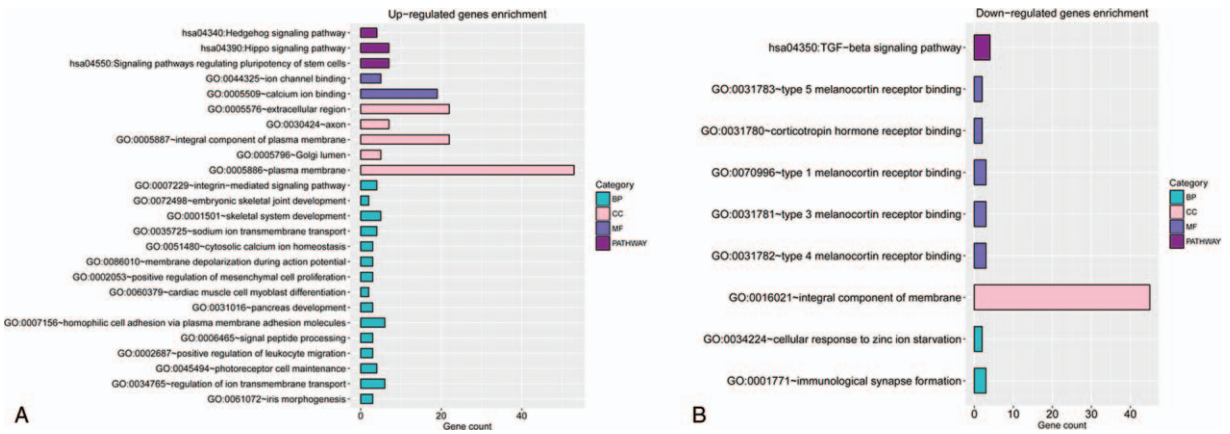

Figure 4. The CC, BP, and MF terms, and Kyoto Encyclopedia of Genes and Genomes pathways enriched with (A) upregulated and (B) downregulated differentially expressed genes. BP = biological process, CC = cellular component, MF = molecular function.

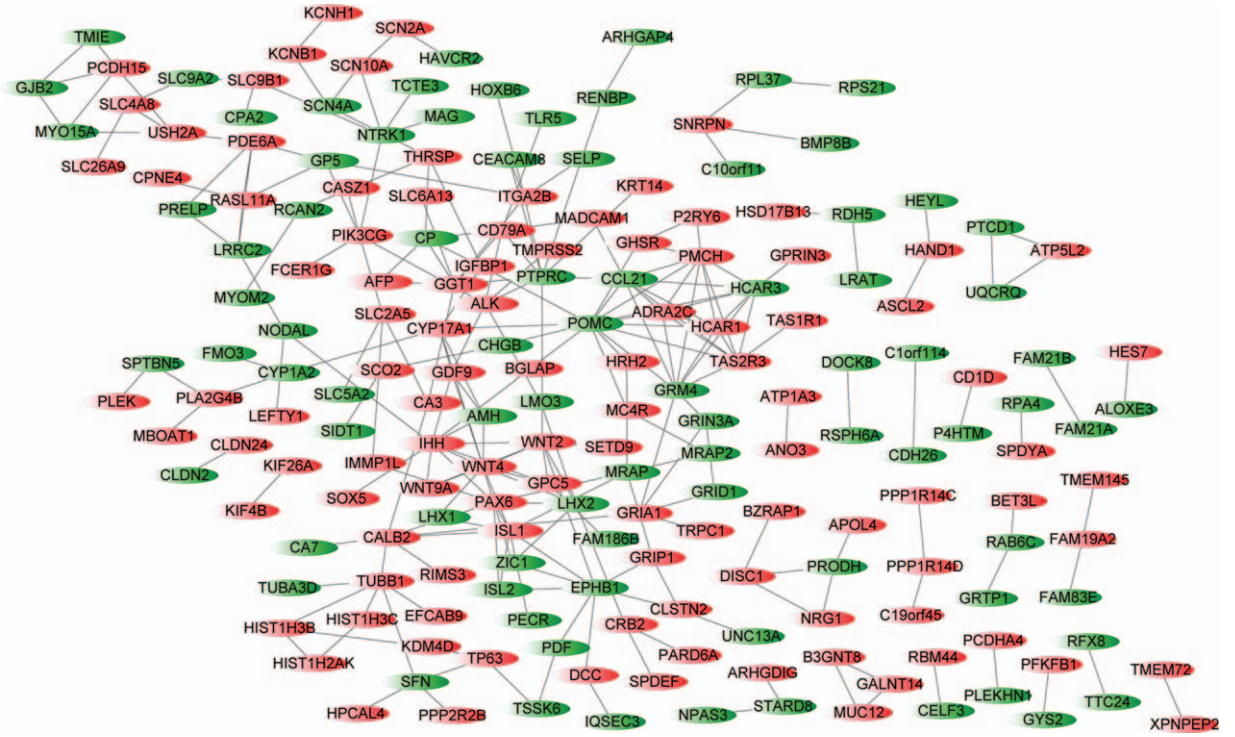

Figure 5. The protein–protein interaction network constructed using the differentially expressed genes. Red nodes represent upregulated genes and green nodes represent downregulated ones.

Recent studies demonstrated an important role for ISL1 in anterior heart field development.[36] Interestingly, *ISL1* was an upregulated DEG in this study; it was also suggested to be strongly linked with functions associated with cardiac muscle cell myoblast differentiation (GO:0060379). ISL1 was first identified as a key regulator of the *rat insulin I* gene enhancer and expressed in the endocrine cells of the pancreas.[37] Recently, it was defined as a marker of the cardiac progenitor cell lineage that can

Table 1

The top 25 nodes with high topology scores that were calculated by 3 centrality methods in protein–protein interaction network.

	Degree		Betweenness		Closeness
POMC	14	CALB2	3352.0713	PTPRC	0.0154723
WNT4	11	PTPRC	3146.6016	WNT4	0.0154635
IHH	10	PIK3CG	2693.1719	IHH	0.0154547
PMCH	9	POMC	2376.8315	WNT2	0.0154409
GRM4	9	TUBB1	2268.8333	PAX6	0.0154346
CCL21	9	CYP17A1	2263.9873	GDF9	0.0154308
PAX6	9	WNT2	2076.281	ALK	0.0154283
PTPRC	9	IHH	2049.132	CYP17A1	0.0154258
TAS2R3	8	ALK	1904.3726	GGT1	0.0154258
HCAR3	8	NTRK1	1817.8857	CALB2	0.0154233
WNT2	8	WNT4	1772.7386	CCL21	0.0154196
ISL1	8	PAX6	1713.1864	POMC	0.0154121
EPHB1	8	EPHB1	1656.1353	ITGA2B	0.0154033
HCAR1	7	GP5	1640.7333	LHX2	0.0154008
ADRA2C	7	PDE6A	1638.0476	ISL1	0.0153983
GRIA1	7	CA3	1551.9026	GRM4	0.0153933
GGT1	7	GGT1	1487.3944	CD79A	0.0153933
CALB2	7	CCL21	1472.4836	CA3	0.0153933
CYP17A1	6	ITGA2B	1451.0048	AMH	0.0153921
LHX2	6	GRIA1	1420.8928	PIK3CG	0.0153921
CD79A	6	USH2A	1402.6143	BGLAP	0.0153821
ITGA2B	6	THRSP	1342.4524	IGFBP1	0.0153759
ALK	6	NODAL	1312.4429	EPHB1	0.0153722
PIK3CG	6	CYP1A2	1238	CP	0.0153722
TUBB1	6	IGFBP1	1111.5037	GRIA1	0.0153684

POMC = proopiomelanocortin, WNT4 = Wnt family member 4.

Table 2

The CC, BP, and MF terms, and KEGG pathways enriched by 15 hub nodes in protein–protein interaction network.

Category	Term	*P*	Genes
BP	GO:0007267~cell–cell signaling	1.15E-03	*WNT2*, *CCL21*, *POMC*, *IHH*
BP	GO:0061072~iris morphogenesis	6.81E-03	*WNT2*, *PAX6*
BP	GO:0061180~mammary gland epithelium development	6.81E-03	*WNT2*, *WNT4*
BP	GO:0001771~immunological synapse formation	8.50E-03	*CCL21*, *EPHB1*
BP	GO:0006702~androgen biosynthetic process	9.35E-03	*CYP17A1*, *WNT4*
BP	GO:0007411~axon guidance	9.69E-03	*PTPRC*, *PAX6*, *EPHB1*, *ITGA2B*
BP	GO:0048596~embryonic camera-type eye morphogenesis	1.10E-02	*PAX6*, *IHH*
BP	GO:0002407~dendritic cell chemotaxis	1.27E-02	*PIK3CG*, *CCL21*
BP	GO:0032967~positive regulation of collagen biosynthetic process	1.94E-02	*WNT4*, *IHH*
BP	GO:0030325~adrenal gland development	1.94E-02	*CYP17A1*, *WNT4*
BP	GO:0002053~positive regulation of mesenchymal cell proliferation	2.36E-02	*WNT2*, *IHH*
BP	GO:0002088~lens development in camera-type eye	2.78E-02	*WNT2*, *PAX6*
BP	GO:0051209~release of sequestered calcium ion into cytosol	3.11E-02	*PTPRC*, *CCL21*
BP	GO:0022008~neurogenesis	3.19E-02	*WNT2*, *EPHB1*
BP	GO:0048666~neuron development	3.28E-02	*ALK*, *IHH*
BP	GO:0070527~platelet aggregation	3.36E-02	*PIK3CG*, *ITGA2B*
BP	GO:0048469~cell maturation	3.53E-02	*CCL21*, *IHH*
BP	GO:0045860~positive regulation of protein kinase activity	3.77E-02	*PTPRC*, *CCL21*
BP	GO:0060326~cell chemotaxis	3.77E-02	*CCL21*, *EPHB1*
BP	GO:0071560~cellular response to transforming growth factor beta stimulus	4.10E-02	*WNT2*, *WNT4*
BP	GO:0045165~cell fate commitment	4.43E-02	*WNT2*, *WNT4*
BP	GO:0045944~positive regulation of transcription from RNA polymerase II promoter	4.55E-02	*WNT2*, *PAX6*, *POMC*, *IHH*
CC	GO:0005615~extracellular space	2.28E-03	*WNT2*, *WNT4*, *CCL21*, *GGT1*, *POMC*, *IHH*
CC	GO:0005886~plasma membrane	4.55E-03	*PIK3CG*, *WNT2*, *PTPRC*, *WNT4*, *GRIA1*, *GGT1*, *EPHB1*, *IHH*, *ITGA2B*
CC	GO:0009986~cell surface	8.12E-03	*PTPRC*, *WNT4*, *GRIA1*, *ITGA2B*
CC	GO:0005578~proteinaceous extracellular matrix	1.57E-02	*WNT2*, *WNT4*, *IHH*
CC	GO:0005576~extracellular region	2.34E-02	*WNT2*, *WNT4*, *CCL21*, *POMC*, *EPHB1*
MF	GO:0048018~receptor agonist activity	1.27E-02	*WNT2*, *WNT4*
MF	GO:0005109~frizzled binding	3.10E-02	*WNT2*, *WNT4*
PATHWAY	hsa04550:Signaling pathways regulating pluripotency of stem cells	2.02E-03	*PIK3CG*, *WNT2*, *WNT4*, *PAX6*
PATHWAY	hsa04340:Hedgehog signaling pathway	3.98E-03	*WNT2*, *WNT4*, *IHH*
PATHWAY	hsa04916:Melanogenesis	1.47E-02	*WNT2*, *WNT4*, *POMC*
PATHWAY	hsa05200:Pathways in cancer	3.43E-02	*PIK3CG*, *WNT2*, *WNT4*, *ITGA2B*

BP = biological process, CC = cellular component, KEGG = Kyoto Encyclopedia of Genes and Genomes, MF = molecular function, POMC = proopiomelanocortin, WNT4 = Wnt family member 4.

differentiate into cardiomyocyte, smooth muscle cell, and endothelialcell lineages of the heart.[38] Cai et al[36] found that Isl1 knockout mice have a severely deformed heart, suggesting the importance of ISL1 in this organ. Therefore, we speculated that miR-3144-5p overexpression may lead to the upregulation of *ISL1*, which in turn plays a role in HCMs.

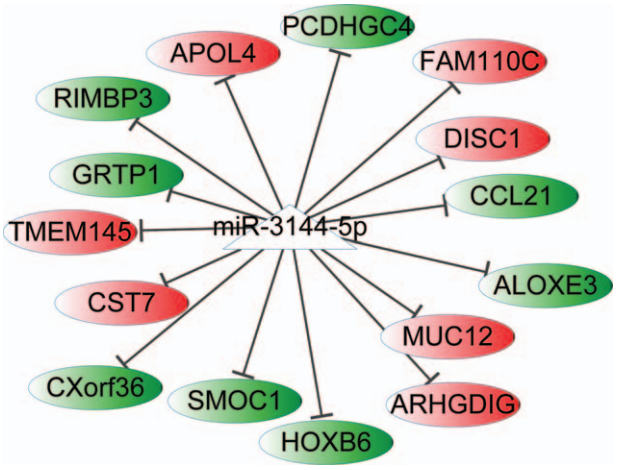

Figure 6. The miR-3144-5p-target gene regulatory network. Red nodes represent upregulated genes and green nodes represent downregulated ones. White triangles represent miRNA.

In addition to *ISL1*, *NRG1* was also suggested to be associated with cardiac muscle cell myoblast differentiation. NRG1 belongs to the neuregulin family, which consists of ErbB1, 2, 3, and 4. NRG1 is also an agonist for receptor tyrosine kinases of the epidermal growth factor receptor family.[39] Studies have found that it is essential for normal development of the nervous system and the heart.[40,41] NRG1 plays multiple roles in cardiovascular biology and has been suggested to be a cardiomyocyte mitogen, stimulating heart muscle cells to divide.[42] Wang et al[43] have reported that NRG1 can induce embryonic stem cells to differentiate into cardiomyocytes. Taking these findings together, miR-3144-5p overexpression may induce NRG1 to regulate the function of HCMs.

Enhanced circulating levels of C-C chemokines reportedly play a pathogenic role in congestive heart failure.[44] In this study, a C-C chemokine, CCL21, was identified to be one of the hub nodes that had high topology scores in 3 centrality methods in the PPI network. Specifically, it was predicted to be a target gene of miR-3144-5p. A study found that CCL21 elicits its effect through binding to a cell surface chemokine receptor, namely C-C chemokine receptor 7.[45] C-C chemokine receptor 7 and its ligands were previously shown to be related to the development of heart failure. Additionally, markedly enhanced CCL21 expression was found within the failing myocardium in human

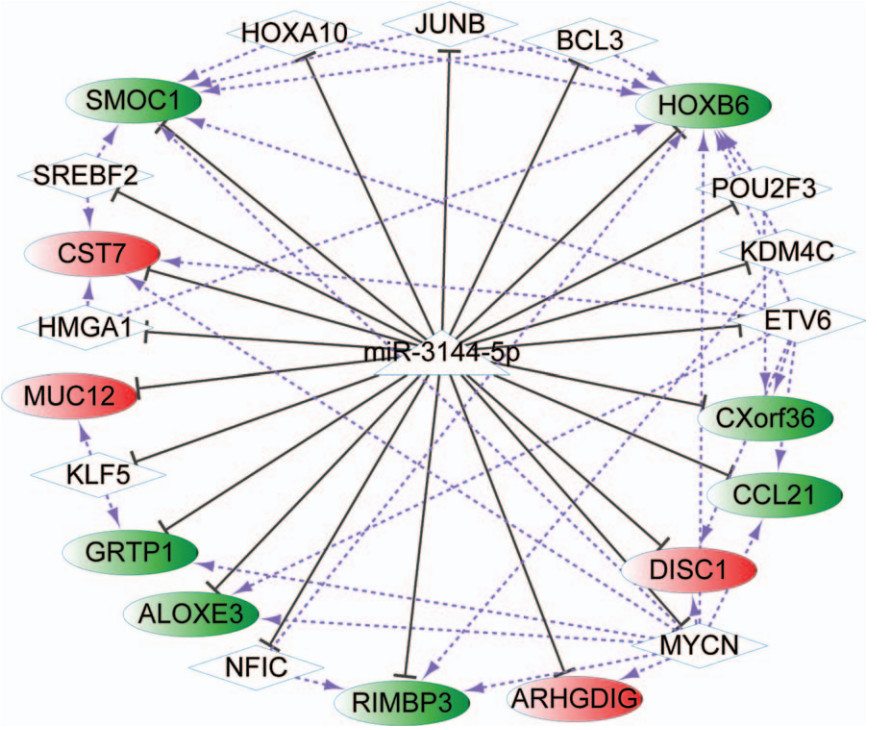

Figure 7. The miR-3144-5p-transcription factor-target gene coregulatory network. Red nodes represent upregulated genes and green nodes represent downregulated ones. White triangles represent miRNA and white rhombuses represent transcription factors. Black solid line represents the regulatory relationship between miR-3144-5p and the target gene. Purple dotted line represents the regulatory relationship between the transcription factor and the target gene.

heart failure. It has served as a potential mediator in myocardial failure.[46] Given the regulatory relationship between miR-3144-5p and *CCL21* and the role of CCL21 in heart failure, we speculated that miR-3144-5p may play a role in the function of HCMs by targeting *CCL21*.

The TF MYCN was included in the miR-3144-5p-TF-target gene coregulatory network, which suggested that miR-3144-5p interacts with MYCN, thereby playing a role in HCMs. MYCN is a member of the MYC family of TFs, with a basic helix–loop–-helix domain. It has to dimerize with another basic helix–loop–-helix protein to bind DNA.[47] Importantly, MYCN has been found to be necessary for the expression of myofilament proteins, which are important for the structure and function of cardiomyocytes. MYCN promotes the proliferation and growth of cardiomyocytes by regulating the expression of cell cycle regulators and p70S6K, respectively.[48] A study also suggested that mutations in MYCN are involved in Feingold syndrome, a disorder associated with congenital heart defects.[49] Taking these findings together, miR-3144-5p may regulate the expression of MYCN to impact the functions of HCMs.

Although so many genes had been predicted to be differentially expressed in HCMs with miR-3144-5p overexpression, the exact expression levels of these DEGs and TF, especially *ISL1*, *NRG1*, *CCL21*, and MYCN were not confirmed in the experimental study. Additionally, due to high cost of high-throughput sequencing, the sample size was usually small. Therefore, our further study will focus on the functional roles of miR-3144-5p as well as the key DEGs in cardiac arrhythmia based on more samples of animal models to validate our results.

In conclusion, *ISL1*, *NRG1*, *CCL21*, and MYCN were differentially expressed in the miR-3144-5p mimic group, which suggested that miR-3144-5p overexpression plays a role in HCMs by regulating the expression of these genes and TF. The findings in this study may provide a new insight into the molecular mechanisms underlying the progression of cardiac arrhythmia.

Acknowledgments

The authors thank The independent innovation research fund of Huazhong University of Science and Technology (Program No.2017KFYXJJ131) and the Specialized Research Fund for the Doctoral Program of Higher Education from the Ministry of Education (Program No.20130142120068) for the support.

References

[1] Wronska A, Kurkowska-Jastrzebska I, Santulli G. Application of microRNAs in diagnosis and treatment of cardiovascular disease. Acta Physiol 2015;213:60.
[2] Jha SK, Karole S. An overview on arrhythmia and its management. 2016.
[3] Santulli G, Iaccarino G, De Luca N, et al. Atrial fibrillation and microRNAs. Front Physiol 2014;5:15.
[4] Teng Y, Zhang R, Liu C, et al. miR-143 inhibits interleukin-13-induced inflammatory cytokine and mucus production in nasal epithelial cells from allergic rhinitis patients by targeting IL13Rα1. Biochem Biophys Res Commun 2014;457:58–64.
[5] Terentyev D, Belevych AE, Terentyeva R, et al. miR-1 overexpression enhances Ca(2+) release and promotes cardiac arrhythmogenesis by targeting PP2A regulatory subunit B56alpha and causing CaMKII-dependent hyperphosphorylation of RyR2. Circ Res 2009;104:514–21.
[6] Nair N, Kumar S, Gongora E, et al. Circulating miRNA as novel markers for diastolic dysfunction. Mol Cell Biochem 2012;376:33–40.
[7] Stark MS, Tyagi S, Nancarrow DJ, et al. Characterization of the melanoma miRNAome by deep sequencing. Plos One 2010;5:e9685.
[8] Hamfjord J, Stangeland AM, Hughes T, et al. Differential expression of miRNAs in colorectal cancer: comparison of paired tumor tissue and adjacent normal mucosa using high-throughput sequencing. Plos One 2012;7:e34150.

[9] Han CNN, Xie W, Ming Y, et al. Expression differences of circulating MicroRNAs in metastastic castration resistant prostate cancer and low-risk, localized prostate cancer. Prostate 2013;73:346.
[10] Xiao F, Zuo Z, Cai G, et al. miRecords: an integrated resource for microRNA–target interactions. Nucleic Acids Res 2009;37:D105–10.
[11] Olesen MS, Jensen NF, Holst AG. A novel nonsense variant in Nav1.5 Cofactor MOG1 eliminates its sodium current increasing effect and may increase the risk of arrhythmias. Can J Cardiol 2011;27:523.e17–23.e23.
[12] Wu L, Yong SL, Fan C, et al. Identification of a new co-factor, MOG1, required for the full function of cardiac sodium channel Nav 1.5. J Biol Chem 2008;283:6968–78.
[13] Tfelt-Hansen J, Winkel BG, Grunnet M, et al. Inherited cardiac diseases caused by mutations in the Nav1.5 sodium channel. J Cardiovasc Electrophysiol 2010;21:107–15.
[14] Nikolayeva O, Robinson MD. edgeR for differential RNA-seq and ChIP-seq analysis: an application to stem cell biology. Methods Mol Biol 2014;1150:45–79.
[15] Robinson MD, McCarthy DJ, Smyth GK. edgeR: a Bioconductor package for differential expression analysis of digital gene expression data. Bioinformatics 2010;26:139–40.
[16] Law CW, Chen Y, Shi W, et al. Voom: precision weights unlock linear model analysis tools for RNA-seq read counts. Genome Biol 2014; 15:R29.
[17] Ritchie ME, Phipson B, Wu D, et al. limma powers differential expression analyses for RNA-sequencing and microarray studies. Nucleic Acids Res 2015;43:e47.
[18] Smyth GK. Limma: linear models for microarray data. Bioinformatics and computational biology solutions using R and bioconductor 2005; Springer:397–420.
[19] Gu Z, Eils R, Schlesner M. Complex heatmaps reveal patterns and correlations in multidimensional genomic data. Bioinformatics 2016;32:2847–9.
[20] Da Wei Huang BTS, Lempicki RA. Systematic and integrative analysis of large gene lists using DAVID bioinformatics resources. Nat Protoc 2008;4:44–57.
[21] Stelzl U, Worm U, Lalowski M, et al. A human protein-protein interaction network: a resource for annotating the proteome. Cell 2005;122:957–68.
[22] Szklarczyk D, Franceschini A, Wyder S, et al. STRING v10: protein–-protein interaction networks, integrated over the tree of life. Nucleic Acids Res 2014;gku1003.
[23] Shannon P, Markiel A, Ozier O, et al. Cytoscape: a software environment for integrated models of biomolecular interaction networks. Genome Res 2003;13:2498–504.
[24] Lim J, Hao T, Shaw C, et al. A protein–protein interaction network for human inherited ataxias and disorders of Purkinje cell degeneration. Cell 2006;125:801–14.
[25] Rito T, Deane CM, Reinert G. The importance of age and high degree, in protein-protein interaction networks. J Comput Biol 2012;19:785–95.
[26] Goh KI, Oh E, Kahng B, et al. Betweenness centrality correlation in social networks. Phys Rev E Stat Nonlin Soft Matter Phys 2003;67(1 Pt 2):017101.
[27] Okamoto K, Chen W, Li X-Y. Ranking of closeness centrality for large-scale social networks. 2008;Frontiers in Algorithmics, Springer:186–195.
[28] Tang Y, Li M, Wang J, et al. CytoNCA: a cytoscape plugin for centrality analysis and evaluation of protein interaction networks. Biosystems 2015;127:67–72.
[29] Dweep H, Gretz N. miRWalk2.0: a comprehensive atlas of microRNA-target interactions. Nat Methods 2015;12:697.
[30] Janky R, Verfaillie A, Imrichová U, et al. iRegulon: from a gene list to a gene regulatory network using large motif and track collections. PLoS Comput Biol 2014;10:e1003731.
[31] Enright AJ, John B, Gaul U, et al. MicroRNA targets in Drosophila. Genome Biol 2003;5:R1.
[32] Novák J, Olejníčková V, Tkáčová N, et al. Mechanistic Role of microRNAs in coupling lipid metabolism and atherosclerosis. 2015; microRNA: Basic Science, Springer:p. 79–100.
[33] Vickers KC, Rye K-A, Tabet F. MicroRNAs in the onset and development of cardiovascular disease. Clin Sci 2014;126:183–94.
[34] Wronska A, Kurkowska-Jastrzebska I, Santulli G. Application of microRNAs in diagnosis and treatment of cardiovascular disease. Acta Physiol 2015;213:60–83.
[35] Shan H, Li X, Pan Z, et al. Tanshinone IIA protects against sudden cardiac death induced by lethal arrhythmias via repression of micro-RNA-1. Br J Pharmacol 2009;158:1227–35.
[36] Cai CL, Liang X, Shi Y, et al. Isl1 identifies a cardiac progenitor population that proliferates prior to differentiation and contributes a majority of cells to the heart. Dev Cell 2003;5:877–89.
[37] Karlsson O, Thor S, Norberg T, et al. Insulin gene enhancer binding protein Isl-1 is a member of a novel class of proteins containing both a homeo-and a Cys–His domain. Nature 1990;344:879–82.
[38] Bu L, Jiang X, Martinpuig S, et al. Human ISL1 heart progenitors generate diverse multipotent cardiovascular cell lineages. Nature 2009;460:113–7.
[39] Fuller SJ, Sivarajah K, Sugden PH. ErbB receptors, their ligands, and the consequences of their activation and inhibition in the myocardium. J Mol Cell Cardiol 2008;44:831–54.
[40] Talmage DA. Mechanisms of neuregulin action. Novartis Found Symp 2008;289:74–86.
[41] Britsch S. The neuregulin-I/ErbB signaling system in development and disease. Adv Anat Embryol Cell Biol 2007;190:1–65.
[42] Gemberling M, Karra R, Dickson AL, et al. Nrg1 is an injury-induced cardiomyocyte mitogen for the endogenous heart regeneration program in zebrafish. eLife 2015;4: e05871.
[43] Wang Z, Xu G, Wu Y, et al. Neuregulin-1 enhances differentiation of cardiomyocytes from embryonic stem cells. Med Biol Eng Comput 2009;47:41–8.
[44] Aukrust P, Ueland T, Müller F, et al. Elevated circulating levels of C-C chemokines in patients with congestive heart failure. Circulation 1998;97:1136–43.
[45] Yoshida R, Nagira M, Kitaura M, et al. Secondary lymphoid-tissue chemokine is a functional ligand for the CC chemokine receptor CCR7. J Biol Chem 1998;273:7118–22.
[46] Yndestad A, Finsen AV, Ueland T, et al. The homeostatic chemokine CCL21 predicts mortality and may play a pathogenic role in heart failure. Plos One 2012;7:1250–67.
[47] Lu X, Pearson A, Lunec J. The MYCN oncoprotein as a drug development target. Cancer letters 2003;197:125–30.
[48] Cristina H, Yin P, Paige DB, et al. Myocardial Mycn is essential for mouse ventricular wall morphogenesis. Dev Biol 2013;373:53–63.
[49] Marcelis CLM, Hol FA, Graham GE, et al. Genotype–phenotype correlations in MYCN-related Feingold syndrome. Hum Mutat 2008;29:1125–32.